THE PULLOUT TEST OF A FRP REBAR WITHIN A NANOCLAY/CONCRETE BLOCK

Wei-Chong Liao, Han-Yang Lin, Meng-Chang Lee and Pai-Heng Hung
Department of Civil Engineering, Feng Chia University
100 Wen Hwa Rd., Taichung, Taiwan
e-mail: wcliao@fcu.edu.tw

SUMMARY

The FRP (fiber reinforced plastic) rebar with good corrosion resistance and high stiffness weight ratio is a good alternative of a steel reinforcement for environmental deterioration prevention. In this study, a filament winding technique is applied to commercially available FRP rods (with smooth surface) to produce different winding pitch and lug height. This simulated lug provides the shear transfer mechanism between the FRP rod and concrete. These FRP rods are embedded in the concrete block during the concrete casting. A pullout test of FRP rebar from the concrete block was performed to examine the shear transfer capacity made from different winding methods. Results show that the bond behavior of FRP rod with longitudinal and oblique angle winding is better than that of a FRP rod with 90 degree winding without axial winding.

Keywords: GFRP rod, filament winding, pullout test

INTRODUCTION

Concrete must be reinforced with materials strong in tension because of its small tensile capacity. Conventionally, concrete has been reinforced with steel reinforcing bars. To transfer the forces from the concrete to the steel reinforcement, a good shear bond must be developed between the concrete and the steel. Steel reinforcing bars are manufactured with deformed surface to enhance shear transfer. In addition, it needs enough embedment length to develop the full capacity of the rebar. However, if the RC structures are exposed to deteriorative environments, it could leads to corrosion of the reinforcing steel. The whole structure might lose its loading capacity and reduce its service life. This urges the researches of finding a substitute for steel rebar or invention of new corrosion prevention technology. The FRP (fiber reinforced plastic) rebar with good corrosion resistance and high stiffness weight ratio will be a good candidate for this purpose. To fully utilize FRP rebars as reinforcement for concrete structure, some attempts have been made. Larralde et. Al.,[1] compared the bond behaviors between the FRP/concrete and steel bar/concrete. Results from pullout tests on FRP and steel rebars in concrete showed that the anchorage design for steel rebars is not directly applicable on FRP rebars. The average nominal bond stress at failure was greater for the steel rebars than for the FRP rebars. The slip of the rebars relative to the concrete surface was greater for the FRP rebars than for the steel rebars. Okelo et. Al. [2] studied the bond strength of fiber reinforced polymer (FRP) rebars in normal strength concrete. Test results showed that the bond strength of an FRP rebar is about 40–100% the bond strength on a steel rebar for pullout failure mode. The bond strength of FRP rebars was also evaluated through the bending test of beam specimens [3]. Bakis, et. Al.[4] investigated the bonding mechanisms of smooth and

lugged FRP rods embedded in concrete. From the experiment, a bond-slip finite element model was established to predict the behavior of environmentally degraded rods. Although there are several researches regarding the bond behavior between the FRP rebar and concrete[5-8], the investigation of GRFP rebar lugs made from filament winding is still few. In this study, a filament winding technique is applied to commercially available FRP rods (with smooth surface) to produce different winding pitch, lug height, and winding angle. This simulated lug will provide the shear transfer mechanism between the FRP rod and concrete. These FRP rods are embedded in the concrete block during the concrete casting. A pullout test of FRP rod from the concrete cylinder was performed to examine the shear transfer capacity made from different winding pitch, lug height, and winding angle. The bond-slip data were recorded during the experiment. The optimum winding method to produce qualified bond for FRP rod are addressed.

THE MANUFACTURING OF A FRP REBAR

In this study, three kinds of winding method were applied to make FRP rebars. The first one employed a spiral winding on the bare FRP rod. A programmed winding angle can control the pitch of the FRP rebars, while the lug height was controlled by the number of winding loops. The lug has an average height of 0.73 mm, lug width of 5.2 mm and lug spacing of 7.62mm. This kind of GFRP rod is designated as the "beta" specimen (the top specimen in Fig. 1). The second method takes several transverse winding, i.e., 90^o wound, at the same place and then moved forward to the next lug according to the designed pitch (the middle specimen in Fig. 1). It revealed that the second method can control the FRP rebar with desirable pitches and lugs. Both approaches wind glass strand on a premade rugged surface FRP rod. There is no axial winding in both methods, and the original FRP rod has a diameter of 9.36 mm to simulate a no. 3 steel rebar. In the third method, the filament winding was applied for GFRP rods with a diameter of 6.35mm. In order to increase the bond between the original pultruded FRP rod and the winding strand, the zero degree wound was first adopted along the longitudinal direction. It is hard to do a 0^o winding using the original mandrel of the winding machine. Therefore a special designed mandrel as shown in Fig. 2 was employed to allow the filament wound in the longitudinal direction. After that, a programmed $\pm 45^o$, 90^o or 60^o helical winding was applied. Table 1 shows the specimen number and the designed lug height and pitch of the GFRP rebar in this experiment. In which "w" stands for the specimen without a 0^o winding, the first three digits is the lug height, and the last two numbers is the lug spacing. After the filament winding all specimens were cured inside a 70℃ oven for two hours.

Fig. 1. GFRP rebars made from different winding methods (top: beta, bottom: Aslan)

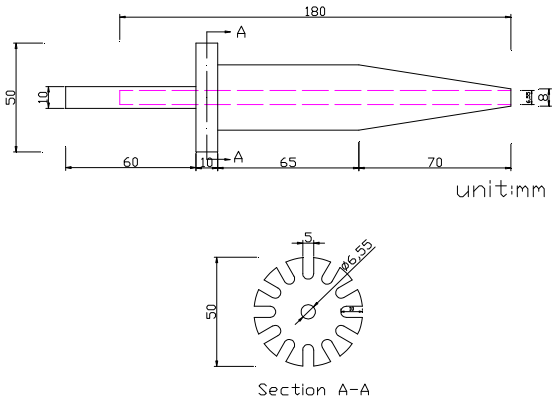

Fig. 2. Mandrel for longitudinal winding

A room temperature cured resin was used during the filament winding process. The RL-300A is the resin which has a viscosity of 15000 cps at 25^oC, and the hardener is RL-300B with a viscosity of 30 cps at he same temperature. The pot life of this epoxy is 2 hrs. The finished

FRP rebars were inserted inside the concrete mould during the casting of concrete cylinders. All concrete specimens have a dimension of ϕ10cm×20cm.

For the concrete composition, type I OPC, river sand, and gravel were used as the basic materials. The gravel has a SSD relative density of 2.61, with water absorption of 1.71%. The maximum diameter of the gravel is 19.1mm.The river sand has a SSD relative density of 2.50, with absorption of 2.04%. The fineness modulus of the fine aggregate was 2.45. The cement has a relative density of 3.15. The designed strength of the concrete specimens is 35MPa. The slump of the concrete cylinders is 16 cm. There was no admixture used in this study. Concrete cylinders were cured according to the ASTM standard C31-83.

THE FRP REBAR PULLOUT TEST

Two PVC sleeves were loosely attached to the top and bottom end of the concrete specimen used as a bond breaker[3,8] between the FRP rebar and the surrounding concrete as shown in Fig. 3. The embedded length for each GFRP rebar was set as 5 cm for all the specimens tested. In order to have the FRP rebar locate at the center of the concrete cylinder, two guided plates with centered holes were designed for the concentric alignment during the casting.

After curing in water for 28 days, the specimens were taken out for the rebar pullout test. Two LVDTs measured the displacements at the loaded and free ends, respectively. The experimental set up is shown in Fig. 4. An MTS 810 with a stoke speed of 1.25mm/min was used to pull the FRP rebars. During the pullout test displacements from the top and bottom ends, and the pull for were recorded. In order to control the pullout force, a confined circular ring was attached beneath the inner side of the top plate to regulate the pull off region (see Fig. 4). The upper surface of the concrete cylinder was capped with a sulfur compound to control the axial alignment before the testing starts.

Fig.3. The PVC sleeves of the GFRP rebars

Fig. 4. The set-up of pullout test

RESULTS AND DISCUSSION

For comparison, the pullout tests of smooth GFRP rebars and GFRP rebars from Hughes Brothers (the Aslan specimens) were also conducted. Figure 5 demonstrates the bond-slip of a smooth GFRP rebar and a beta specimen. It is seen that the beta specimen can have a maximum bond stress of 8MPa, but it drops at a slip of 1mm. This is due to the smallest lug height of this winding method. Part of the lugs was sheared off at this moment. However, after a slip of 2mm, the bond regains the strength, since the remained lugs can resist the shear off forces. The smooth FRP rod only has a maximum bond stress of 2 MPa, and after the peak

stress, it slips all the way through. Fig. 6 shows the bond-slip at the loaded end and free end of na-14015-1 specimen. Since the lug height of this specimen is larger than that of a beta specimen, it can sustain higher pull force and has a lower bond stress drop after the peak bond stress.

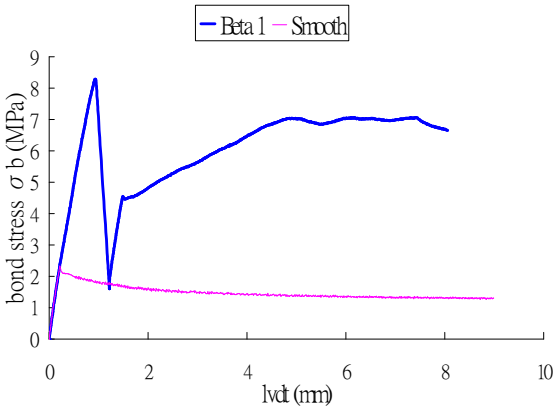

Fig. 5. The bond slip of a smooth FRP bar and a beta specimen.

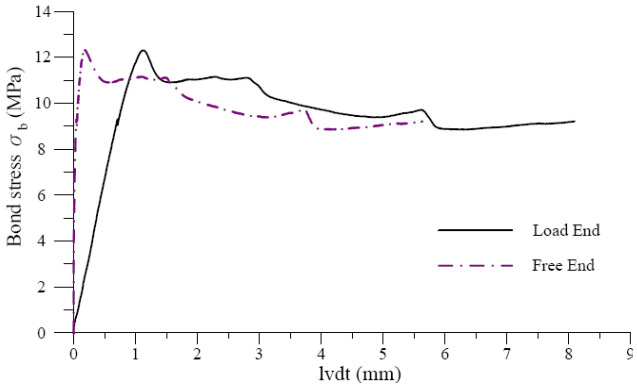

Fig. 6. The bond-slip of GFRP na-14015-1 specimen

The bond stresses under the same lug spacing but different lug height is shown in Figs. 7 and 8. It is seen that the bond stress will increase with the lug height. Table 2 shows the ultimate bond stresses of GFRP rebars without axial windings. As the lug height increase some of the specimens exhibits larger bond stress than the Aslan specimen. For example, the maximum bond stresses of the w19615-3 and w14020-2 specimens are 22.8% and 18.9% greater than that of the Aslan specimen, respectively. However, from Figs 7 and 8, the post-peak bond stress loss was greater than that of the Aslan. This might due to that the filament winding was performed on the existing FRP rod, so the bond between the FRP rod and the winding strand forms a weak link at large shear force. If the filament winding was conducted during the pultrusion of the FRP rod, a less steep post peak behavior can be achieved. Table 3 is the ultimate bond stress for GFRP rebars made by method 3. The 60^o helical/axial winding has higher bond stress than the Aslan rebar. Although the 08920-1 specimen with axial/transverse wound has a lower maximum bond stress than the w-08420 specimen with transverse wound, the post peak bond stress drop is small. Some specimens show a flat plateau after the peak bond stress. Fig. 9 depicts the bond slip of a 60^o helical/axial wound specimen. The bond stress drop after the peak is negligible. It reveals that the helical/axial bound method creates a better bond at the interface of the FRP core and the winding strand.

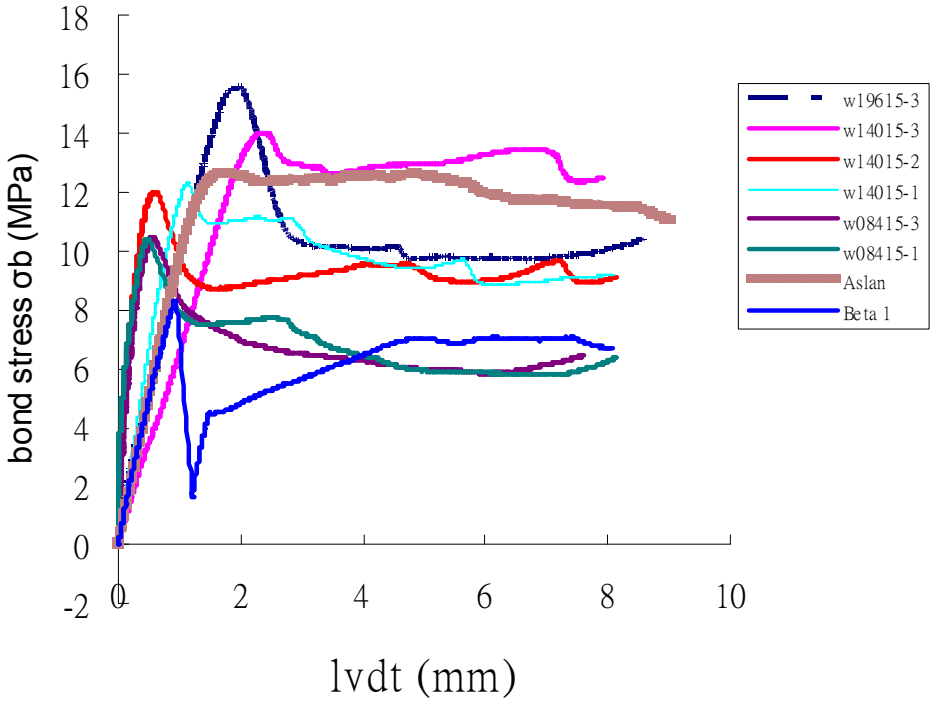

Fig. 7. Bond stress at different lug heights lug (pitch=15mm)

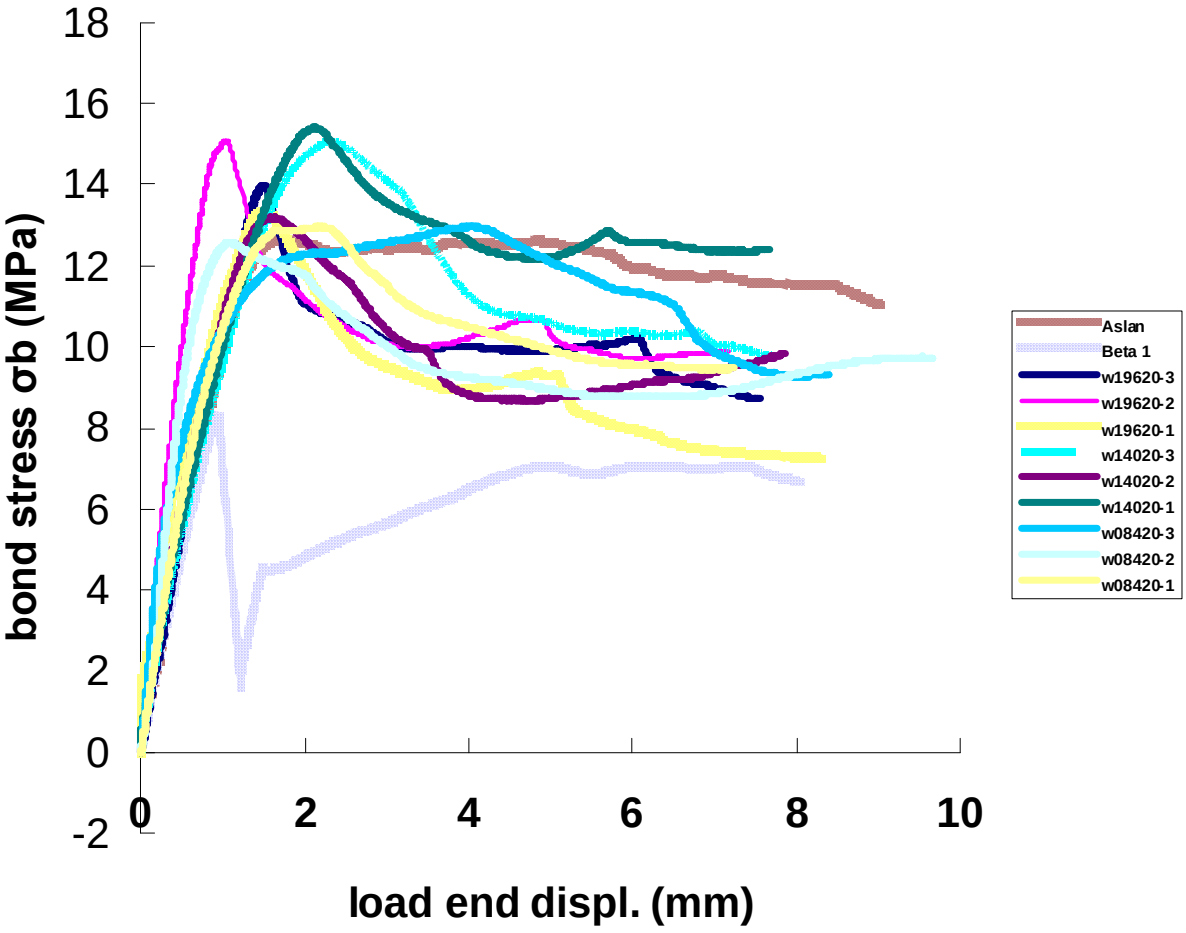

Fig. 8. Bond stress at different lug heights lug (pitch=20mm)

Table 1 The filament winding design specifications of GFRP rods

Specimen	Axial winding	Winding angle	Lug pitch (mm)	Lug height (mm)
beta	no	spiral	5.2	0.73
w-08415	no	90^o	15	0.84
w-08420			20	
w-14015			15	1.40
w-14020			20	
w-19615			15	1.96
w-19620			20	
45	yes	$\pm 45^o$	33.05	0.75
60		$\pm 60^o$	20.00	0.96
08920		90^o	20	0.89
14515			15	1.45
14520			20	1.45
19620			20	1.96

Table 2 The ultimate bond stresses for FRP rebars without axial winding

specimen	Ultimate bond stress (MPa)	Difference to Aslan (%)	specimen	Ultimate bond stress (MPa)	Difference to Aslan (%)
w-08415-1	10.4	-18.1	w-08420-1	13.0	2.4
w-08415-2	10.5	-17.3	w-08420-2	13.0	2.4
w-14015-1	12.3	-3.1	w-14020-1	15.4	21.3
w-14015-2	12.0	-5.5	w-14020-2	15.1	18.9
w-19615	15.6	22.8	w-19620-1	15.1	18.9
Aslan	12.7		w-19620-2	14.0	10.2

Table 3 The ultimate bond stresses for FRP rebars without axial winding

specimen	Ultimate bond stress (MPa)	Difference to Aslan (%)	specimen	Ultimate bond stress (MPa)	Difference to Aslan (%)
45-1	11.9	-6.3	08920-1	11.5	-9.4
45-2	10.5	-17.3	08920-2	11.3	-11.0
60-1	13.6	7.1	08920-3	11.5	-9.4
60-2	14.4	13.4	14520-1	11.6	-8.7
60-3	15.1	18.9	14520-2	12.0	-5.5
Aslan	12.7		14520-3	13.0	2.4

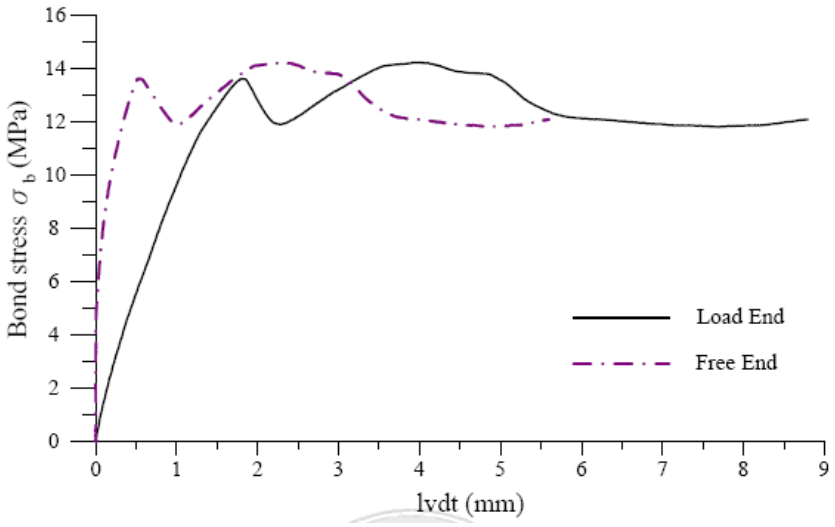

Fig. 9. The bond-slip of a 60^o helical/axial winding GFRP rebar.

A lug/GFRP failure for the transverse/no axial wound is shown in Fig. 10. It happens at the interface of the lug and GFRP bar. Since the transverse wound was made on an existing FRP rod, and the lugs have less fiber volume fraction than the original FRP rod which will form a weakest link during the pullout test. Figure 11 shows the failure of a helical/axial wound specimen. A V-shaped gap between the loaded end and the first lug is seen.

Fig. 10. Failure mode of a transverse/no axial wound specimen

Fig. 11. Failure mode of a helical/ axial wound specimen

CONCLUSIONS

Three kinds of filament winding method were adopted in this study to make artificial lugs for the FRP rod to simulate the behavior of a steel rebar. The pullout tests evaluate the bond stress for GFRP rebars made by these methods. From the experiment, it can be concluded that:

Most of the failure happens at the lug/ core GFRP interface of transverse/no axial wound specimens. Because the lugs were made from the filament wound of an existing FR bar the lug/FRP interface will form a weakest link during the pullout test. For transverse wound specimens with 15mm lug spacing, the bond stress increases with the lug height. The bond stress drop for helical/axial wound specimen is less than that of a transverse/no axial wound specimen. If a helical winding can be performed just before the set of a pultruded FRP rod, the FRP rebar will have a better bond stress.

ACKNOWLEDGEMENTS

Partial supports from the National Science Council, Taiwan, under grants NSC 97-2221-E-035-080 is acknowledged.

References

1. Larralde, J.; Silva-Rodriguez, R., "Bond and slip of FRP rebars in concrete ," Journal of Materials in Civil Engineering, v 5, n 1, p 30-40, Feb, 1993

   Okelo, Roman; Yuan, Robert L., "Bond strength of fiber reinforced polymer rebars in normal strength concrete," Journal of Composites for Construction, v 9, n 3, p 203-213, May/June 2005
2. Okelo, Roman, "Realistic bond strength of FRP rebars in NSC from beam specimens ," Journal of Aerospace Engineering, v 20, n 3, p 133-140, 2007
3. Bakis, C.E.; Uppuluri, V.S.; Nanni, A.; Boothby, T.E., "Analysis of bonding mechanisms of smooth and lugged FRP rods embedded in concrete," Composites Science and Technology, v 58, n 8, p 1307-1319, August 1998
4. Saadatmanesh, H. and Ehsani, R. M., "Application of Fiber Composites in Civil Engineering," Proceedings, Structures Congress, Structural Materials, J. F. Orofino, Ed., ASCE, New York, 1989, pp. 526-535.
5. Larralde, J., Renbaum, L., and Morsi, A., "Fiberglass Reinforced Plastic Rebars in Lieu of Steel Rebars," Proceedings, Structures Congress, Structural Materials, J. F. Orofino, Ed., ASCE, New York, 1989, pp. 261-269.
6. Larralde, J. and Silva-Rodriguez, R., "Bond and Slip of FRP Rebars in Concrete," Journal of Materials in Civil Engineering, Vol. 5, No. 1, February 1993, pp. 30-40.
7. Larralde, J. and Silva-Rodriguez, R., Burdette, J., and Harris, B., "Bond Tests of Fiberglass-Reinforced Plastic Bars in Concrete," Journal of Testing and Evaluation, Vol. 22, No. 4, July 1994, pp. 351-359.
8. Antonio Nanni, Masaharu Tanigaki, and Koichi Hasuo, "Bond Anchorage of Pretensioned FRP Tendon at Force Release," Journal of Structural Engineering, Vol. 118, No. 10, October, 1992. Paper No. 2491. pp.2837-2854.